Wave-induced flicker level emitted by a tidal farm

Anne Blavette, Bernard Multon, Hamid Ben Ahmed, Lukas Morvan, Alice Verschae, Mohamed Machmoum, Dara O 'Sullivan

Wave-induced flicker level emitted by a tidal farm

Anne Blavette
Bernard Multon
Hamid Ben Ahmed
SATIE, ENS-Rennes
France
anne.blavette@gmail.com

Lukas Morvan
Alice Verschae
French Navy
France

Mohamed Machmoum
IREENA
University of Nantes
France

Dara O'Sullivan
Analog Devices
Cork
Ireland

***Abstract*—The inherently fluctuating nature of sea waves can be reflected to a significant extent in the power output of tidal turbines. However, these fluctuations can give rise to power quality issues such as flicker. Hence, it is important to assess the impact which tidal farms may have on their local network before such power plants are allowed to connect to the grid. This paper describes the influence of the wave climate on the short-term flicker level induced by a tidal farm on the point of common coupling. It analyses also under which conditions the tidal farm breaches the grid code requirements in terms of short-term flicker level.**

***Index Terms*—tidal energy, flicker, wave, grid code**

I. INTRODUCTION

Tidal turbines are now considered as sufficiently mature to be deployed in pre-commercial tidal farms [1]-[2]. So far, they have been tested in sheltered areas where the influence of sea waves on their power output could be considered as negligible [3]. Hence, wave-induced flicker generated by tidal turbines has not been analyzed experimentally, nor has it been studied numerically, despite the significant influence waves may have on the electrical power output of a tidal turbine [4]. This paper intends to fill this gap in simulating the flicker level generated by a tidal farm by means of numerical power system simulations.

II. MODELING

A. Tidal Turbine Characteristics

The characteristics of the tidal turbine considered in this study were extracted from [4] and are summarized in Table I. The turbine is equipped with a permanent magnet synchronous generator.

B. Modeling of the Horizontal Water Speed

The mechanical power extracted by a tidal turbine is calculated based on the horizontal component V of the water flow speed perpendicular to the rotation plane of its blades. This horizontal speed is composed of contributions from the tidal current and from the waves. It must be noted that interactions between these two phenomena may result in a significant increase of the mean wave height [5]. However, these interactions are still not fully understood. In addition, they are currently modeled for detailed turbine structural design analyses at a relatively basic level in the ideal case of monochromatic waves superimposed to a linear tidal current [6]. Hence, it was deemed reasonable for the power system simulations performed in this study not to model these interactions at a first stage in similar fashion to [4]. Consequently, the horizontal component V of the water flow speed at any point in space and time can be formulated as:

$$V(x,z,t) = U_t(z,t) + U_w(x,z,t) \quad (1)$$

where x and z are the horizontal and the vertical axes respectively, t is the time, U_t and U_w are the speed contributions from the tidal current and from the waves respectively. The most unfavorable case of collinear speed contributions is considered here.

TABLE I. TIDAL TURBINE CHARACTERISTICS

Parameter	Name	Numerical value
R	Turbine radius	8 m
J	System total inertia	$1.3131.10^6$ kg.m²
P_n	Generator nominal power	1.5 MW
p	Pole pair number	120
ψ_m	Permanent magnet flux	2.458 Wb
R_s	Generator stator resistance	0.0081 Ω
L_d, L_q	Generator *d*-*q* axis inductances	1.2 mH
f_g	Grid frequency	50 Hz
d_h	Water depth at hub height	22 m

1) Tidal current contribution U_t

The tidal flow is considered as linear and perpendicular to the rotation plane $(0yz)$ of the turbine blades. Hence, no turbulence effect is considered in this study. It is important to recall that, although this phenomenon may induce a significant level of flicker [3], the objective of this study consists in analyzing wave-induced flicker only.

The variation of the tidal flow speed U_t at the sea surface (z=0 m) as a function of time is usually considered as sinusoidal for diurnal tides such as:

$$U_t(0,t) = U_{t,max}\sin\left(\frac{2\pi t}{T_t}\right) \quad (2)$$

where $U_{t,max}$ is the maximum tidal current speed selected arbitrarily as equal to 3.5 m/s in this study. This value is typical of high speed tidal currents characterizing the areas where tidal farms are envisaged to be deployed. Term T_t is the tidal period almost equal to half a lunar day, i.e. 12h25 ≈ 44,700 seconds. The variations of the tidal flow speed as a function of the water depth z ($z < 0$) for a given time t_0, can be modeled as follows [7]:

$$U_t(z,\ t_0) = U_t(0,t_0)\left(\frac{d+z}{d}\right)^{1/7} \quad (3)$$

where d is the distance between the sea surface and the sea bottom which is equal to 35 m in this study. This water depth corresponds to this of the site selected for the Paimpol-Bréhat tidal farm in France [4]. In summary, the contribution in speed U_t from the tidal current can be expressed as:

$$U_t(z,t) = U_{t,max}\sin\left(\frac{2\pi t}{T_t}\right)\left(\frac{d+z}{d}\right)^{1/7} \quad (4)$$

2)Waves contribution U_w

Sea surface elevation is usually modeled using linear wave theory [8]. However, this theory is not valid for shallow to intermediate waters which are traditionally characterized by a water depth less than 50 m, as it is the case in this study. Stokes' wave theory is the typical alternative for modeling non-linear waves in shallow to intermediate waters. The order of Stokes' law must be selected based on the wave climate characteristics considered, i.e. the significant wave height H_s and the peak period T_p, and on the water depth d. The significant wave height H_s is the height of the one-third of the highest waves of a sea-state and the peak period T_p is the period corresponding to the frequency band Δf with the maximum value of spectral density in the non-directional wave spectrum $S(f)$ characterizing a given sea-state. A classical Bretschneider spectrum was selected. It is defined as [8]:

$$S(f) = \frac{5H_s^2}{16T_p^4}\frac{1}{f^5}e^{-\frac{5}{4T_p^4 f}} \quad (5)$$

In this study, the significant wave height range considered is 2 m ≤ H_s ≤8 m and the peak period range considered is 5 s ≤ T_p ≤15 s. These values correspond to wave climates having low to high energy levels.

It appears clearly from Fig. 1 that the waves can be modelled as 2nd order Stokes waves for the cases considered in this study. In the case of a monochromatic wave of height H and of period T, the velocity potential ϕ can thus be expressed as [10]:

$$\phi = \frac{HL}{2T}\frac{ch\big(k(d+z)\big)}{sh(kd)}\sin(kx-\omega t) + \frac{3\pi^2H^2}{16T}\frac{ch\big(2k(d+z)\big)}{sh^4(kd)}\sin\big(2(kx-\omega t)\big) \quad (6)$$

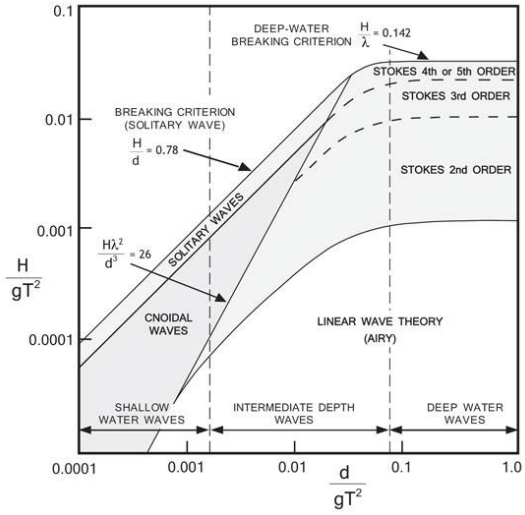

Figure 1. Domains of validity of several wave theories (after [9])

where k is the wave number defined as $k = 2\pi/L = \omega/\sqrt{gd}$ [8] ω the radian frequency defined as $\omega = 2\pi f$. Hence, the contribution in speed U_{w_i} on the x (horizontal) axis from a single monochromatic wave can be calculated as:

$$U_{w_i}(x,z,t) = \frac{\partial\phi}{\partial x} = \frac{\pi H}{T}\frac{ch\big(k(d+z)\big)}{sh(kd)}\cos(kx-\omega t) + \frac{3\pi^2H^2}{4TL}\frac{ch\big(2k(d+z)\big)}{sh^4(kd)}\cos\big(2(kx-\omega t)\big) \quad (7)$$

However, a sea-state is the sum of multiple waves of amplitude a_i, of period T_i and of wave number k_i. Hence, the total contribution in speed U_w of all the monochromatic waves is the sum of their individual contributions U_{w_i} such as:

$$U_w(x,z,t) = \sum_i U_{w_i}(x,z,t) = \sum_i \frac{2\pi a_i}{T_i}\frac{ch\big(k_i(d+z)\big)}{sh(k_i d)}\cos(k_i x-\omega_i t) + \frac{3\pi^2 a_i^2}{T_i L_i}\frac{ch\big(2k_i(d+z)\big)}{sh^4(k_i d)}\cos\big(2(k_i x-\omega_i t)\big) \quad (8)$$

The amplitudes a_i are calculated such as [8]:

$$a_i = \sqrt{2S(f_i)\Delta f} \quad (9)$$

3)Averaged water flow speed

As it will be explained in the next section, the mechanical power extracted by the tidal turbine depends on the cube of the water flow speed $\overline{V(t)}$ averaged over the circular surface swept by the blades. This variable can be calculated as:

$$\overline{V(t)} = \frac{\int_{-d_h-R}^{-d_h+R} V(x,z,t)2\sqrt{R^2-(d_h+z)^2}\,dz}{\pi R^2} \quad (10)$$

Profiles for the average speed $\overline{V(t)}$ were simulated for four values of the significant wave height H_s: 2 m, 4 m, 6 m, 8 m,

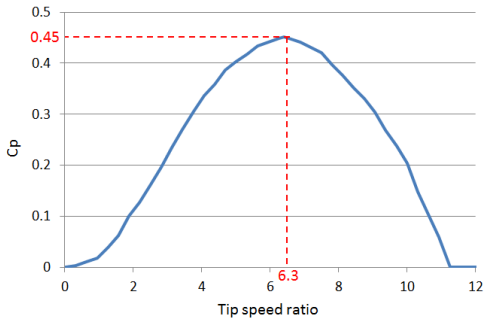

Figure 2. Power coefficient C_p as a function of the tip speed ratio λ

and for four values of the peak period T_p: 5 s, 7 s, 9 s, 11 s, 13 s, 15 s.

C. Modeling of the Tidal Turbine

The mechanical power P_{mec} extracted by the tidal turbine can be expressed as:

$$P_{mec}(t) = \frac{1}{2}\rho\pi R^2 C_p\left(\overline{V(t)}\right)^3 \qquad (11)$$

where ρ is the density of sea water equal to 1027 kg/L and C_p is the power coefficient. The curve of the optimal power coefficient C_p as a function of the tip speed ratio λ considered in this study was extracted from [4] and is reproduced in Fig. 2. The tidal turbine is controlled in speed so that the power coefficient C_p remains sufficiently close to its maximal value. The control system was developed under Matlab-Simulink and is shown in Fig. 3. The mechanical power P_{mec} extracted by the tidal turbine is computed based on the rotor speed and on the C_p-λ characteristic of the turbine in the "Power extraction" block. This block computes also the dynamic reference speed $\omega_{ref}(t)$ to maintain power coefficient C_p close to its maximal value. The error between the dynamic reference speed $\omega_{ref}(t)$ and the rotor speed is transformed into phase voltages to be applied at the terminals of the turbine. The blocks "dq2abc" and "PWM inverter" were extracted from Simulink model "power_pmmotor.mdl" which simulates field-oriented control [11]. The *d*-*q* axes inductances L_d and L_q are equal and the generator has permanent magnet excitation so the control of the electrical torque T_e relies solely on the quadrature axis current i_q. The direct axis current i_d is maintained at zero.

D. Modeling of the Tidal Farm

The electrical power output P_{tot} of an entire tidal farm composed of 20 turbines was simulated based on the addition of identical individual electrical power profiles P_{e_n} (where n=[1, …, 20]) each shifted by a random time delay δ_n. The tidal turbines are assumed to be operated at unity power factor, thus leading to a farm nominal power S_n equal to 20×1.5=30 MVA.

E. Modeling of the Electrical Network

The electrical network was modeled under power system simulator PowerFactory [12] as shown in Fig. 4. It is composed of (from right to left): a "static generator" built-in model outputting the electrical power output P_{tot} of the tidal farm, a 0.4/10 kV transformer, a 1 km long submarine cable whose length was selected arbitrarily, a 0.1 MVA load (load 1), a 5 km long overhead line, a VAr compensator to maintain the power factor at the point of common coupling (PCC) at unity, a 20/38 kV transformer, a 2 MVA load (load 2) and finally a 15 Ω impedance in series with a constant 38 kV voltage source simulating the rest of the national grid. This model is inspired from a model already used in previous works [13] and representing the Irish marine energy test site, called AMETS, located off Belmullet [14]. Short-term flicker was evaluated by means of a flickermeter compliant with IEC standard 61000-4-15 [15].

III. Results

A. Influence of the Wave Climate on the Flicker Level

1) Significant wave height H_s

Fig. 5 presents the flicker level P_{st} as a function of significant wave height H_s for different impedance angles Ψ_k and different peak periods T_p. It appears clearly that the significant wave height H_s has a considerable influence on the flicker level P_{st}. However, this influence is highly dependent on the impedance angle Ψ_k. This can be explained by means of the simple two-bus system shown in Fig. 6. The generator G connected to Bus 1 injects a complex power $P + jQ$ (where j is the imaginary unit) into to the impedance

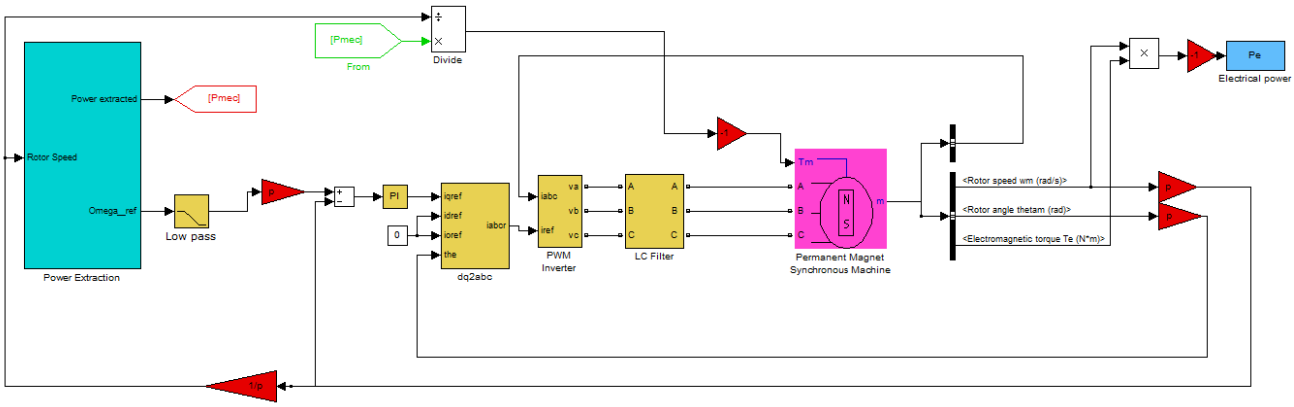

Figure 3. Speed control system developed under Matlab-Simulink

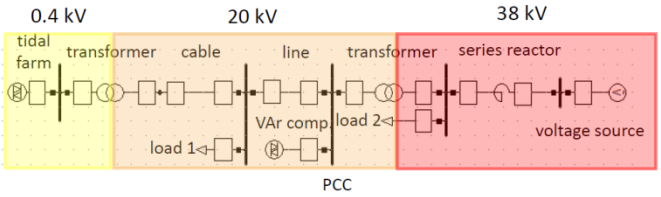

Figure 4. Electrical network modeled under PowerFactory

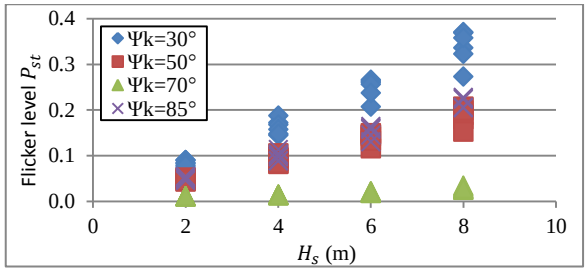

Figure 5. Flicker level P_{st} as a function of significant wave height H_s for different impedance angles Ψ_k and different peak periods T_p

$R_{eq} + jX_{eq}$ connected in series with a constant voltage source simulating an infinite grid. The energy transport results in both active and reactive power consumption in the impedance which increases with the amount of active power P injected. Hence, the impedance acts as a load. Its reactive power consumption is supplied by the constant voltage source which acts as a slack bus. This case can be approximated qualitatively to the classic two-bus system connected by a lossless line, provided that the active and reactive power consumption of the impedance is transferred to generator G. In this case, the voltage deviation $\Delta V = V_1 - V_2$ can be formulated as:

$$\Delta V = \frac{PR_{eq}+QX_{eq}}{V_1} \qquad (12)$$

Hence, for sufficiently low impedance angles Ψ_k (i.e. resistive networks), the voltage deviation ΔV is influenced mostly by the active power P. On the contrary, for sufficiently high impedance angles Ψ_k (i.e. reactive networks), the influence of the reactive power Q dominates.

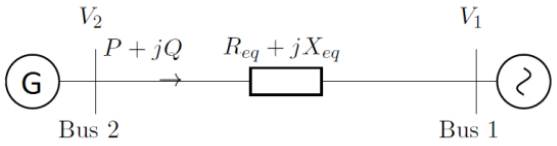

Figure 6. Simple two-bus system

In similar fashion, the influence of the active power P_{tot} generated by the farm decreases as a function of the impedance angle Ψ_k, as it is more and more reduced by the opposite influence of the reactive power flow to the series reactor, the 20/38 kV transformer and the 38kV load. Hence, the amplitude of the voltage variations initially induced by the tidal farm decreases up to Ψ_k=70°, thus resulting in a lower flicker level. However, the influence of the reactive power flow is predominant for Ψ_k=85°, which leads to an increase of the voltage fluctuations amplitude, thus to a higher flicker level.

2) Peak period T_p

It can be observed from Fig. 5 that the peak period T_p has a non-negligible, though more limited influence on the flicker level P_{st} than the significant wave height H_s. However, as it can be observed in Fig. 6, there is no trivial relation between the flicker level P_{st} and the peak period T_p. This was expected due to the low level of coupling between the speed fluctuations induced by the waves and the individual electrical power output P_e of each turbine due to their large inertia J. In a previous work focusing on wave energy devices [16], it had been demonstrated that the flicker level induced by a wave farm including no means of storage could be reasonably well estimated by means of a sinusoidal voltage profile whose period was equal to the sea-state energy period (which is proportional to the peak period T_p used here). However, this method was no longer applicable in the case where a significant storage capacity was included in the wave farm. In similar fashion, the large inertia of tidal turbines acts as a storage means of considerable energy capacity.

B. *Compliance of the tidal farm with flicker requirements*

In order to maintain the quality of the electricity supplied to the customer, grid operators require that any grid-connected installation complies with a certain number of requirements, and among them flicker requirements. In most grid codes, flicker is required to be maintained under a maximal allowed limit at the PCC. Numerical values found in a number of national grid codes range between 0.35 and 1 for short-term flicker [13]. In order to perform an analysis independent of the short-circuit level S_k of the rest of the national grid, the flicker coefficient $c_f(\Psi_k)$ was used. This coefficient is expressed as [17]:

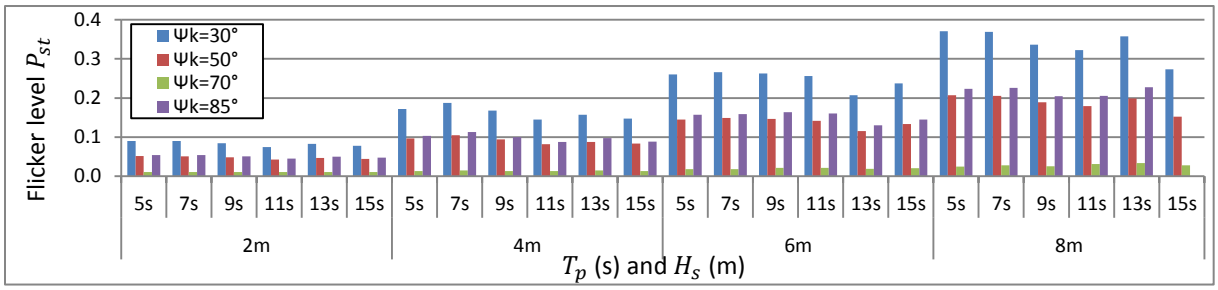

Figure 7. Flicker level P_{st} as a function of the peak period T_p and of the significant wave height H_s for different impedance angles Ψ_k

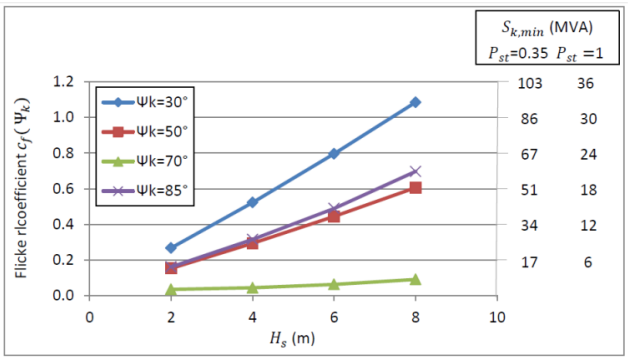

Figure 8. Flicker level P_{st} as a function of the peak period T_p

$$c_f(\Psi_k) = P_{st}\frac{S_k}{S_n} \quad (13)$$

For a given impedance angle Ψ_k, the flicker coefficient $c_f(\Psi_k)$ is constant. Fig. 8 shows the flicker coefficient $c_f(\Psi_k)$ as a function of the significant wave height H_s for different impedance angles Ψ_k. The minimum short-circuit level $S_{k,min}$ for which the flicker level P_{st} remains below the maximum allowed flicker level limit $P_{st,max}$ is calculated such as:

$$S_{k,min} = \frac{c_f(\Psi_k)S_n}{P_{st,max}} \quad (14)$$

Numerical values of the minimum short-circuit level $S_{k,min}$ are shown on the right-hand side of Fig. 8. They correspond to the values of the flicker coefficient $c_f(\Psi_k)$ indicated on the left-hand side axis of the graph. The values for $S_{k,min}$ were calculated for each of the maximum allowed flicker limits considered in this study and equal to 0.35 and 1.0 respectively. It can be observed that the minimum short-circuit level $S_{k,min}$ for which the flicker level P_{st} remains below unity is relatively close to the nominal power of the tidal farm. Considering that it is unlikely that a 30 MW tidal farm may be envisaged to be connected to such nodes due to power transmission capacity issues, the flicker level P_{st} can be considered as unlikely to exceed the most permissive limit. The same observations apply to most situations in the case of the most stringent flicker limit equal to 0.35. However, this limit may be exceeded in the rare cases meeting the three following conditions: 1) the tidal farm is connected to a node of relatively low short-circuit level in the range of approximately 50 MVA to 100 MVA, 2) the tidal farm is operated in highly energetic wave conditions (H_s≥6 m), which is quite unlikely, 3) the impedance angle Ψ_k of the grid node to which the tidal farm is connected is less than or equal to 50°, or equal to 85°. Hence, based on these observations, it can be concluded that the flicker level induced by a tidal farm on its local network is unlikely to exceed even the most stringent flicker limit. It is important to point out that the influence of no other storage means (e.g. batteries, supercapacitors) than the tidal turbine inertia was included in the model. However, this study has also shown that flicker could reach significant levels. This could contribute to make the total flicker level induced by the tidal farm and other installations connected to the same node exceed the maximum allowed limit in the case where the pre-connection flicker is already significantly high.

IV. Conclusions

This paper has described the influence of sea waves on the quality of the electrical power output generated by a tidal farm in terms of short-term flicker level P_{st}. First, the influence of the wave climate characteristics (significant wave height H_s and peak period T_p) on the flicker level P_{st} was studied. Then, the compliance of the tidal farm with the grid code requirements in terms of short-term flicker level was also analyzed in the second part of this paper. It was shown that the flicker level P_{st} induced by the tidal farm at the point of common coupling is unlikely to exceed even the most stringent limit found among a number of national grid codes. However, the flicker induced by the tidal farm reaches significant levels. Hence, in the case where the pre-connection flicker level is already significant, the grid connection of a tidal farm may lead the total flicker level at the point of common coupling to exceed the maximum allowed limit.

References

[1] EDF, Tidal farm of Paimpol-Bréhat, France, http://energie.edf.com

[2] RITE project, Verdant Power, http://www.verdantpower.com

[3] J. MacEnri, M. Reed, and T. Thiringer, "Influence of tidal parameters on SeaGen flicker performance", *Phil. Trans. R. Soc. A*, vol. 371, no. 1985, February 2013.

[4] Z. Zhou, F. Scuiller, J. Charpentier, M. El Hachemi Benbouzid and T. Tang, "Power Smoothing Control in a Grid-Connected Marine Current Turbine System for Compensating Swell Effect", *IEEE Trans. on Sustainable Energy*, vol. 4, pp. 816-826, July 2013.

[5] A. Saruwatari, D. Ingram and L. Cradden, "Wave-current interaction effects on marine energy converters", *Ocean Engineering*, vol. 73, pp. 106-118, 2013.

[6] P. Galloway, L. Myers, A. Bahaj, "Quantifying wave and yaw effects on a scale tidal stream turbine", *Renewable Energy*, vol. 63, pp. 297- 307, 2014.

[7] B. Multon, *Marine Renewable Energy Handbook*, Wiley, 2013.

[8] J. Falnes, *Ocean Waves and Oscillating Systems: Linear Interactions Including Wave-Energy Extraction*, Cambridge University Press, 2002.

[9] B. Le Méhauté, *An Introduction to Hydrodyanmics and Water Waves*, Berlin: Springer-Verlag, 1976.

[10] M. Brorsen, "Non-linear Waves", Lecture notes, Aalborg University, 2007.

[11] L.-A. Dessaint and R. Champagne, "Permanent Magnet Synchronous Machine", Matlab-Simulink model, R2014b.

[12] DIgSILENT PowerFactory, http://www.digsilent.de/

[13] A. Blavette, D. O'Sullivan, R. Alcorn, T. Lewis and M. Egan, "Impact of a Medium-Size Wave Farm on Grids of Different Strength Levels", *IEEE Trans. on Power Systems*, vol. 29, pp. 917 – 923, March 2014.

[14] AMETS test site, www.seai.ie, accessed on 2014/11/21.

[15] *IEC Flickermeter - Functional and design specifications*, standard 61000-4-15, ed2.0, 2010.

[16] A. Blavette, R. Alcorn, M. Egan, D. O'Sullivan, M. Machmoum and T. Lewis, "A novel method for estimating the flicker level generated by a wave energy farm composed of devices operated in variable speed mode", in *Proc. Int. Conf. EVER14*, Monaco, March 2014.

[17] *IEC Measurement and assessment of power quality characteristics of grid connected wind turbines*, standard 61400-21, ed2.0, 2008.